ELSEVIER

International Journal of Mass Spectrometry 222 (2003) 465–479

International Journal of Mass Spectrometry

www.elsevier.com/locate/ijms

Protonation thermochemistry of β-alanine An evaluation of proton affinities and entropies determined by the extended kinetic method

In-Su Hahn, Chrys Wesdemiotis*

Department of Chemistry, The University of Akron, Akron, OH 44325, USA

Received 21 May 2002; accepted 7 October 2002

Dedicated to Professor J.L. Beauchamp on the occasion of his 60th birthday for his innovative and stimulating contributions to gas phase ion chemistry and mass spectrometry.

Abstract

The extended kinetic method is employed to determine the proton affinity (PA) of β-alanine and four other difunctional molecules that can develop intramolecular hydrogen bonds after protonation, including α-alanine and three α,ω-diaminoalkanes. Proton-bound dimers of each of these molecules (AA) and reference bases of similar protonation entropy (B_i) are formed by fast atom bombardment ionization and the dissociation kinetics of the AA–H^+–B_i ions into the individual protonated monomers are assessed as a function of internal energy using tandem mass spectrometry and low energy collisionally activated dissociation (CAD). This procedure accounts for any difference in the activation entropies of the competitive dissociations, $\Delta(\Delta S^{\ddagger})$, which is assumed to be negligible in the conventional kinetic method (one internal energy), thereby leading to more accurate PA data. The proton affinities derived for α-Ala ($902 \pm 4\,kJ\,mol^{-1}$) and 1,2-diaminoethane ($951 \pm 4\,kJ\,mol^{-1}$), i.e., difunctional molecules that form relatively weak hydrogen bonds after protonation, are in excellent agreement with literature values. A PA of $927 \pm 4\,kJ\,mol^{-1}$ is found for β-Ala, the substantial rise vs. PA(α-Ala) reflecting an increased intrinsic basicity upon moving the electron-withdrawing COOH group further away from the amine group and an improved hydrogen bonding arrangement with the β-substitution pattern. The PAs measured for 1,3-diaminopropane ($978 \pm 4\,kJ\,mol^{-1}$) and 1,4-diaminobutane ($993 \pm 4\,kJ\,mol^{-1}$), which develop markedly stronger hydrogen bonds after protonation, are 9 and $13\,kJ\,mol^{-1}$, respectively, lower than reported data. The underestimation is attributed to small reverse barriers and/or an underestimation of $\Delta(\Delta S^{\ddagger})$. Our measurements confirm that the $\Delta(\Delta S^{\ddagger})$ parameter obtained by the extended kinetic method is not a thermodynamic quantity equal to the relative protonation entropy between AA and B_i, but a relative entropy between the dissociating transition states at the actual, generally non-Boltzmann energy distribution of the AA–H^+–B_i heterodimers. Recommendations are given, when to apply the extended kinetic method (involving activation entropy corrections) vis-à-vis its conventional variant. (Int J Mass Spectrom 222 (2003) 465–479)

Keywords: Proton affinities; Kinetic method; Activation entropies; Amino acids; Diamines

* Corresponding author. E-mail: wesdemiotis@uakron.edu

1387-3806/02/$ – see front matter © 2002 Elsevier Science B.V. All rights reserved.
PII S1387-3806(02)01018-7

1. Introduction

Proton attachment significantly influences the structure and function of peptides and proteins in solution [1]. It also is the most important mode of ionization of such molecules in the gas phase, prior to mass spectrometry analysis [2–4]. The biological activity of a protonated peptide and its fragmentations in the gas phase are affected by the proton location, which in turn is partly determined by the intrinsic proton affinities of the peptide's amino acid constituents. For this reason, a large number of mass spectrometry studies have been devoted to establishing the proton affinities of the 20 common α-amino acids [5,6]. In contrast, limited data are available about β-amino acids, although these molecules are encountered in both natural peptides and peptide drugs [7,8]. Lebrilla and co-workers have assessed the gas phase basicity of β-alanine (Scheme 1) using bracketing methods [9]. The present study determines the proton affinity (PA) of this prototype β-amino acid by an expanded version of the Cooks kinetic method [10,11] which also considers entropy effects [12,13].

Proton affinity determinations by the kinetic method start with the formation of proton-bound dimers between the molecule of interest (for example, amino acid AA) and a set of reference bases (B_i). The relative rates of dissociation of the proton-bound dimers to the individual protonated monomers (Eqs. (1a) and (1b)), are obtained through tandem mass spectrometry (MS/MS) experiments. The abundance ratio between the $AA–H^+$ and $B_i–H^+$ fragments in the MS/MS spectrum of $AA–H^+–B_i$ is assumed to be identical to the rate constant ratio, k/k_i, of the competitive dissociations producing these fragments (branching ratio).

$$AA–H^+–B_i \xrightarrow{k} AA–H^+ + B_i \quad (1a)$$

$$AA–H^+–B_i \xrightarrow{k_i} AA + B_i–H^+ \quad (1b)$$

$$\ln\left(\frac{k}{k_i}\right) = \frac{-[\Delta G^{\ddagger}_{(1a)} - \Delta G^{\ddagger}_{(1b)}]}{RT_{eff}} = -\frac{\Delta(\Delta H^{\ddagger})}{RT_{eff}} + \frac{\Delta(\Delta S^{\ddagger})}{R} \quad (2)$$

According to transition state theory [14,15], the natural logarithm of the branching ratio of competing unimolecular reactions is a function of the free energies of activation of these reactions (cf. Eq. (2)), where R is the ideal gas constant and T_{eff} the effective temperature of the energized dimer ions; the free energy term includes relative activation enthalpy and relative activation entropy components, as shown in Eq. (2). An effective instead of an actual temperature is used, because the $AA–H^+–B_i$ dimers probed do not have a Boltzmann distribution of internal energies and are not in thermal equilibrium with their surroundings. T_{eff} represents the temperature of a hypothetical Boltzmann distribution of $AA–H^+–B_i$ ions that fragment to yield the branching ratio observed in the MS/MS spectrum [16–18]. T_{eff} is not a thermodynamic quantity, i.e., one referring to a system in thermal equilibrium and with a Boltzmann energy distribution; it can be viewed as the excess energy per oscillator in the reacting dimer ions [19,20] and has been shown to depend on the size, structure and average binding energy of the dimer, as well as on experimental conditions [16–22].

$$-\Delta(\Delta H^{\ddagger}) = -[\Delta H_{(1a)} - \Delta H_{(1b)}] = PA(AA) - PA(B_i) \quad (3)$$

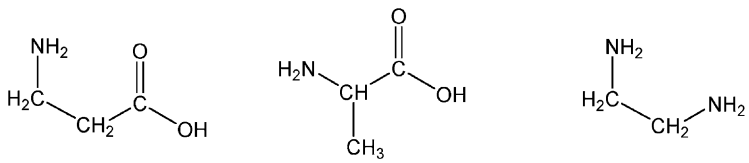

β-alanine α-alanine diaminoethane

Scheme 1.

$$\ln\left(\frac{k}{k_i}\right) = \frac{PA(AA) - PA(B_i)}{RT_{eff}} + \frac{\Delta(\Delta S^{\ddagger})}{R} \quad (4)$$

$$\ln\left(\frac{k}{k_i}\right) \approx \frac{PA(AA) - PA(B_i)}{RT_{eff}} \quad (5)$$

If reactions (1a) and (1b) proceed with no reverse activation energies, the relative enthalpy of activation becomes equal (but with opposite sign) to the relative PA of the molecules compared in the dimer (cf. Eq. (3)), and Eq. (2) is converted to Eq. (4), which relates the experimentally measured branching ratios to relative proton affinities. For dimer ions composed of chemically similar bases (e.g., both amines), the activation entropies of channels (1a) and (1b) are very similar and $\Delta(\Delta S^{\ddagger}) \approx 0$; under these conditions, Eq. (4) is simplified to Eq. (5), the classical version of the kinetic method [10,11]. For many molecules, including β-Ala, however, chemically similar reference bases do not exist. This problem is bypassed by using the extended kinetic method [12,13,23–35], where the reference bases selected are chemically different from the molecule of interest (AA) but similar among each other, so that $\Delta(\Delta S^{\ddagger})$ remains approximately constant within the AA–H^+–B_i series of heterodimers.

$$\ln\left(\frac{k}{k_i}\right) = \left[\frac{PA(AA)}{RT_{eff}} + \frac{\Delta(\Delta S^{\ddagger})}{R}\right] - \frac{PA(B_i)}{RT_{eff}} \quad (6)$$

$$\frac{GB^{app}(AA)}{RT_{eff}} = \frac{PA(AA)}{RT_{eff}} + \frac{\Delta(\Delta S^{\ddagger})}{R} \quad (7)$$

$$\ln\left(\frac{k}{k_i}\right) = \frac{GB^{app}(AA)}{RT_{eff}} - \frac{PA(B_i)}{RT_{eff}} \quad (8)$$

With this requirement satisfied, Eq. (4) is transformed to Eq. (6), in which all parameters that remain constant within the B_i series are enclosed in brackets. The term in brackets represents an apparent gas phase basicity of AA, defined in Eq. (7) [13]. Combination of Eqs. (6) and (7) yields Eq. (8), known as the extended version of the kinetic method. Plotting $\ln(k/k_i)$ vs. $PA(B_i)$ for a series of AA–H^+–B_i dimers gives a regression line whose slope and *y*-intercept provide $1/RT_{eff}$ and $GB^{app}(AA)/RT_{eff}$, respectively (cf. Eq. (8)). Repeating this experiment at several effective temperatures, for example by acquiring MS/MS spectra as a function of collision energy, leads to a set of slopes and intercepts, which can now be plotted against each other (intercepts on *y*-axis). Based on Eq. (7), the new regression line delivers PA(AA) from its slope and $\Delta(\Delta S^{\ddagger})$ from its *y*-intercept.

$$\ln\left(\frac{k}{k_i}\right) = \frac{GB^{app}(AA) - PA(B_i)_{avg}}{RT_{eff}} - \frac{PA(B_i) - PA(B_i)_{avg}}{RT_{eff}} \quad (9)$$

$$\frac{GB^{app}(AA) - PA(B_i)_{avg}}{RT_{eff}} = \frac{PA(AA) - PA(B_i)_{avg}}{RT_{eff}} + \frac{\Delta(\Delta S^{\ddagger})}{R} \quad (10)$$

The described procedure has a serious shortcoming; the parameters $1/RT_{eff}$ and $GB^{app}(AA)/RT_{eff}$ plotted against each other are obtained from the same regression line, viz. Eq. (8). Consequently, they are correlated and the new regression lines obtained from such data suffer from artificially high (almost perfect) correlation coefficients and may lead to underestimated experimental uncertainties [30]. Armentrout has shown that the severity of this problem is abated if the experimental data, i.e., $\ln(k/k_i)$, are plotted vs. $PA(B_i) - PA(B_i)_{avg}$, i.e., vs. the proton affinities of the reference bases relative to their average value, as shown in Eq. (9) [30]. The slopes and *y*-intercepts of Eq. (9) give $1/RT_{eff}$ and $[GB^{app}(AA) - PA(B_i)_{avg}]/RT_{eff}$, respectively. If the latter intercepts are plotted vs. the corresponding slopes, one obtains $PA(AA) - PA(B_i)_{avg}$ from the slope and $\Delta(\Delta S^{\ddagger})$ from its *y*-intercept of the new regression line (cf. Eq. (10)). The error limits of the final results are determined by both the uncertainty in slope and intercept of the two plots [30] as well as the uncertainty in $PA(B_i)$ [31].

Here, we test the described procedure with α-Ala and 1,2-diaminoethane (Scheme 1), whose proton affinities and protonation entropies are well known [5,6], before applying the method to β-Ala, for which no pertinent experimental or theoretical data exist. Amino acids α-Ala and β-Ala are isomers, differing in the position of their functional groups (geminal in α-Ala vs. vicinal in β-Ala); on the other hand,

β-Ala and 1,2-diaminoethane carry vicinal, but different functional groups (Scheme 1). This comparison allows us to assess the effect of compositional and geometrical changes on the thermochemistry of proton attachment.

An additional goal of this investigation is to evaluate the $\Delta(\Delta S^{\ddagger})$ term obtained via the extended kinetic method for proton-bound dimers dissociating without reverse barriers. Earlier studies from our group equated $\Delta(\Delta S^{\ddagger})$ to the thermodynamic entropy difference between the products of reactions (1a) and (1b) which is numerically identical (opposite sign) with the relative entropy of protonation of the bases compared in the dimer, i.e., $\Delta(\Delta S^{\ddagger}) = -\Delta(\Delta S_{H}) = -[\Delta S_{H}(AA) - \Delta S_{H}(B_i)]$ [13]; a similar assumption was made for $\Delta(\Delta S^{\ddagger})$ values deduced from metal ion-bound dimers [24–27]. Laskin and Futrell indeed found very good agreement between these quantities in simulations using either RRKM or finite heat bath theory [36]. In contrast, a more recent microcanonical analysis of the extended kinetic method by Ervin [22] showed that the relative entropy obtained via Eqs. (6)–(8) is neither $-\Delta(\Delta S_{H})$ nor the (very similar) thermodynamic entropy difference between the transition states of reactions (1a) and (1b), but the relative entropy of the latter *transition states at the actual* (*and most likely non-Boltzmann-like*) internal energy distribution of the dissociating ions. The present study provides new information on this subject through the examination of the test molecules α-Ala and 1,2-diaminoethane, whose protonation entropies are well known [5,6]. In this context, we also examined 1,3-diaminopropane and 1,4-diaminobutane, which have significantly larger protonation entropies than the other test molecules [5,6,28,29] and for which experiments by Holmes and co-workers, suggested that their proton-bound dimers with amines may dissociate with significant reverse barriers [29].

2. Experimental

The experiments were performed with a modified Micromass AutoSpec-Q tandem mass spectrometer of EBEhQ geometry (E, electric sector; B, magnetic sector; h, hexapole collision cell; Q, quadrupole). The sector part [37] was used to mass-select the desired proton-bound dimer (MS-1) for collisionally activated dissociation (CAD) in the hexapole collision cell; the fragment ions produced in this process were subsequently mass-analyzed by scanning the quadrupole mass filter (MS-2).

Heterodimers $AA–H^+–B_i$ were produced by fast atom bombardment (FAB) ionization, using ∼12 keV Cs^+ as bombarding particles and glycerol as matrix. The matrix, acidified with a few droplets of trifluoroacetic acid, was saturated with the compound under study (AA) and the reference base (B_i), and 1–2 μL of the resulting solution were applied onto the sample holder and introduced into the FAB ion source. The secondary ions generated upon FAB were accelerated to 8.0 keV before mass selection of $AA–H^+–B_i$ by MS-1. After exiting MS-1, the selected $AA–H^+–B_i$ precursor ion was decelerated to a laboratory frame kinetic energy (E_{lab}) of <100 eV and entered the hexapole collision cell which was pressurized with Ar (5×10^{-7} mbar). E_{lab} is related with the corresponding center-of-mass collision energy (E_{cm}) by the formula $E_{cm} = m/(m + M)$, where m is the mass of the collision gas (40 u) and M the mass of $AA–H^+–B_i$; E_{cm} equals the maximum internal energy available for CAD [38]. The E_{cm} energies employed ranged between 3.5 and 8.9 eV. The fragments formed via CAD in the collision cell were dispersed through MS-2, detected and recorded in the respective CAD mass spectrum (50–100 summed scans). CAD spectra of each $AA–H^+–B_i$ ion were acquired at six different collision energies, and the reproducibility of relative abundances in these spectra was better than ±5%.

A few $AA–H^+–B_i$ dimers were also subjected to metastable ion (MI) analysis in the EBE section of the instrument, in order to determine the kinetic energy releases accompanying the formation of $AA–H^+$ and $B_i–H^+$ fragments [39]. For this, the 8.0 keV $AA–H^+–B_i$ ions were mass-selected by EB and allowed to dissociate spontaneously in the field-free region between the magnet and the second electric sector. The fragments formed there were mass-separated through

the latter sector and recorded in MI spectra composed of ca. 100 summed scans. Kinetic energy releases were calculated from peak widths at half height after correction for the main beam width [39,40]; the energy resolution adjusted in these experiments corresponded to a main beam width at half height of 4.0 V.

The samples (α-alanine, β-alanine and α,ω-diamines), reference bases (amines and amino acids) and trifluoroacetic acid were purchased from Sigma Chemical Co. (St. Louis, MO) and were used as received. The compounded uncertainties of the plots according to Eq. (10), which take into account the standard deviations of slope/intercept from both Eqs. (9) and (10), were calculated by a program provided by Peter B. Armentrout (University of Utah).

3. Results and discussion

3.1. Reference base selection

The extended version of the kinetic method requires that the selected B_i set consists of chemically similar molecules with similar protonation entropies, so that $\Delta(\Delta S^{\ddagger})$ remains approximately constant. B_i must also be chosen such that the AA–H^+–B_i dimers dissociate to yield both protonated monomers, AA–H^+ and B_i–H^+, with detectable intensities. The gas phase basicities of AA and B_i should not differ too much from each other (>50 kJ mol^{-1}), otherwise the k/k_i ratio (i.e., the ratio of the monomer ion abundances) may be irreproducible. Further, it is desirable that GB(AA) be bracketed by the B_i members. The reference bases found to fulfill these conditions were the amines and amino acids listed in Table 1 along with their reported proton affinities and gas phase basicities (at 298 K). The B_i series paired with each of the molecules investigated and the corresponding average proton affinities, $PA(B_i)_{avg}$, and protonation entropies, $\Delta S_H(B_i)_{avg}$, are included in Table 1.

3.2. Dissociations and structures of AA–H^+–B_i

The low energy CAD spectra of all AA–H^+–B_i heterodimers examined in this study (E_{cm} < 10 eV) contain the AA–H^+ and B_i–H^+ fragment ions expected from the competitive dissociations (1a) and (1b). This

Table 1
Average proton affinities (kJ mol^{-1}) and protonation entropies (J mol^{-1} K^{-1}) of the reference base sets (B_i) used in AA–H^+–B_i heterodimers with α-alanine, β-alanine and α,ω-diamines

AA	B_i (PA/GB)[a]	$PA(B_i)_{avg}$	$\Delta S_H(B_i)_{avg}$[b]
β-Alanine	*n*-Propylamine (917.8/883.9), *n*-hexylamine (927.5/893.5), *t*-butylamine (934.1/899.9), imidazole (942.8/909.2); or cysteine (903.2/869.3), valine (910.6/876.7), threonine (922.5/888.5), methionine (935.4/901.5)	930.6 917.9	113.9 113.9
α-Alanine	Propargylamine (887.4/853.5), methylamine (899.0/864.5), allylamine (909.5/875.5), benzylamine (913.3/879.4); or glycine (886.5/852.2), cysteine (903.2/869.3), aspartic acid (908.9/875.0), valine (910.6/876.7)	902.3 902.3	114.1 114.4
1,2-Diaminoethane	*n*-Hexylamine (927.5/893.5), imidazole (942.8/909.2), diethylamine (952.4/919.4), di-*n*-propylamine (962.3/929.3); or threonine (922.5/888.5), methionine (935.4/901.5), tryptophan (948.9/915.0)	946.3 935.6	112.1 113.9
1,3-Diaminopropane	di-*n*-Propylamine (962.3/929.3), di-*n*-butylamine (968.5/935.3), 2,2,6,6,-tetramethylpiperidine (987.0/953.9); or diethylmethylamine (971.0/940.0), triethylamine (981.8/951.), tri-*n*-propylamine (991.0/960.1)	972.6 981.3	111.1 103.7
1,4-Diaminobutane	Triethylamine (981.8/951.), tri-*n*-propylamine (991.0/960.1), tri-*n*-butylamine (998.5/967.6)	990.4	103.6

All data from [6].
[a] Proton affinity (PA) and gas phase basicity at 298 K (GB) in kJ mol^{-1}.
[b] $\Delta S_H(B_i)$ calculated from GB and PA based on the relationship $GB = PA - T\Delta S_H$ (T = 298 K). The standard deviation of the ΔS_H values within each B_i set (a measure of their similarity) is ≤1.7 J mol^{-1} K^{-1}.

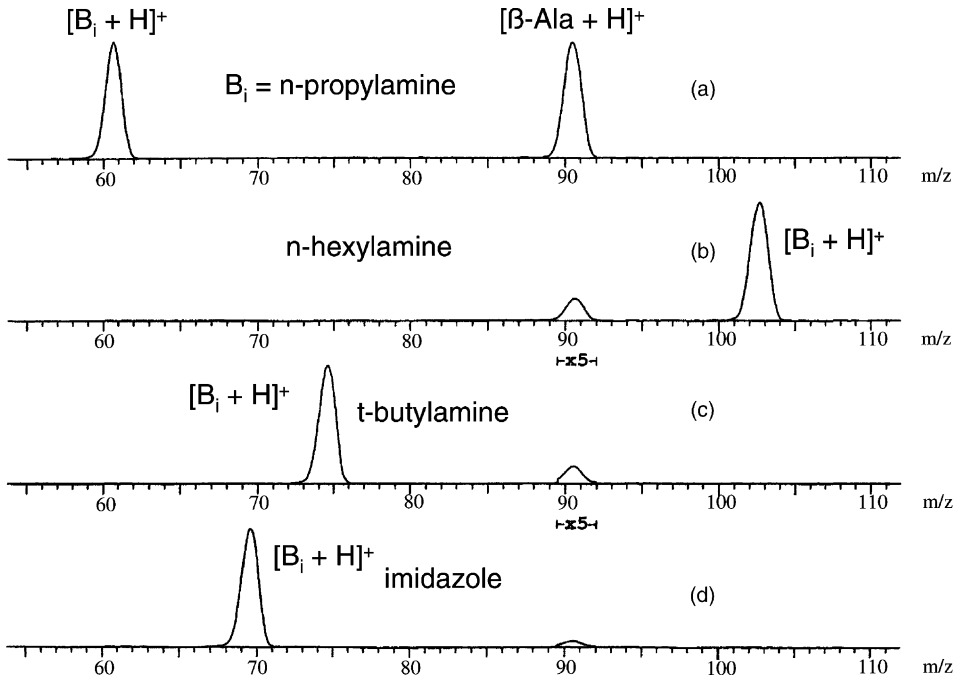

Fig. 1. CAD mass spectra of β-Ala–H^+–B_i heterodimers (B_i = *n*-propylamine, *n*-hexylamine, *t*-butylamine, imidazole) at a center-of-mass collision energy of 6.4 eV.

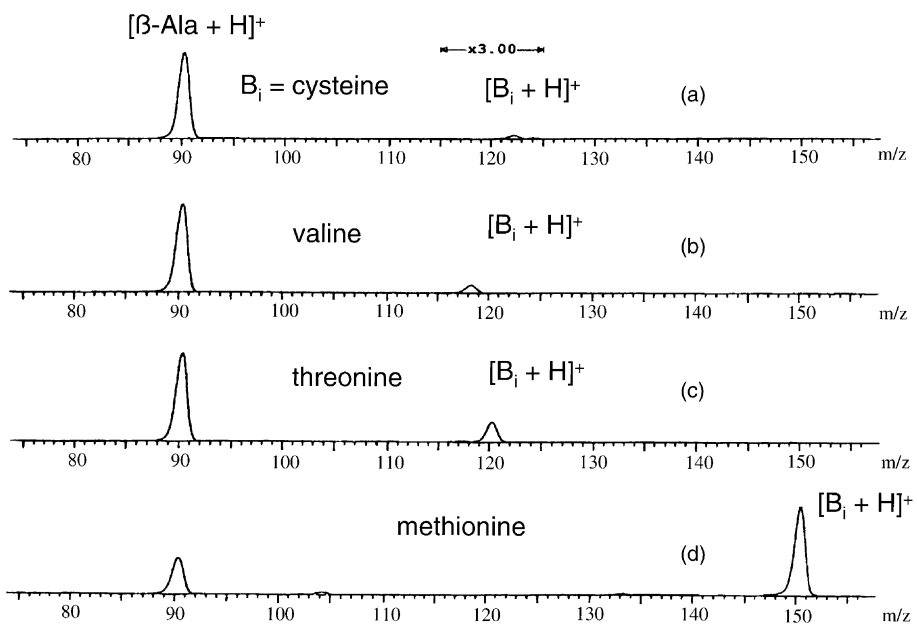

Fig. 2. CAD mass spectra of β-Ala–H^+–B_i heterodimers (B_i = cysteine, valine, threonine, methionine) at a center-of-mass collision energy of 5.4 eV.

is demonstrated in Figs. 1 and 2 for two β-Ala–H^+–B_i sets containing the amine and amino acid reference bases listed in Table 1. No other significant fragment is observed, consistent with the proposed structure, in which the two bases are bridged through the proton.

AA–H^+ and B_i–H^+ also are the dominant fragments in the MI spectra of 8.0 keV AA–H^+–B_i. In this kinetic energy regime and with an energy analyzer for mass separation of the fragment ions, the shapes and widths of the fragment ion signals are very sensitive to the dissociation mechanism [38–40]. In dissociations proceeding with appreciable reverse barriers, a portion of the reverse activation energy is released into translational modes upon decomposition, causing peak broadening and, often, flat- or dish-topped peak shapes; the kinetic energies released in such reactions, calculated from peak widths at half height ($T_{0.5}$), generally exceed 50 meV. On the other hand, in the absence of reverse barriers, the fragment peaks have gaussian shape and small widths ($T_{0.5} < 30$ meV). The AA–H^+ and B_i–H^+ signals from metastable AA–H^+–B_i are consistently gaussian-shaped and narrow; for example, the $T_{0.5}$ values for the β-Ala–H^+ and Thr–H^+ products from metastable β-Ala–H^+–Thr are 16 and 20 meV, respectively. Such results suggest that the investigated proton-bound dimers decompose to the protonated monomers without reverse barriers (as required in uses of the kinetic method for the derivation of thermochemical data); the veracity of this conclusion is discussed later.

3.3. Proton affinities of molecules studied

Detailed experimental data will be presented for β-alanine, which was the focus of our investigation. The CAD spectra of β-Ala–H^+–B_i dimers (B_i = amines or amino acids) were measured at six different collision energies. A plot of the branching ratios in these spectra according to Eq. (9) leads to regression lines, such as the one shown in Fig. 3 which was constructed from CAD spectra of amine-containing heterodimers acquired at $E_{cm} = 6.4$ eV (Fig. 1). The negative slopes ($1/RT_{eff}$) and intercepts ($[GB^{app}(\beta\text{-Ala}) - PA(B_i)_{avg}]/RT_{eff}$) of these lines are summarized in Tables 2 and 3, together with the corresponding standard deviations. Increases in collision energy consistently raise T_{eff}, as expected (vide supra), and also affect $GB^{app} - PA(B_i)_{avg}$ due to the dependence of GB^{app} on T_{eff} (cf. Eq. (7)). When the intercepts of Eq. (9) are plotted against the respective negative slopes, the regression lines of Fig. 4 result, which according to Eq. (10) have slopes $PA(AA) - PA(B_i)_{avg}$ and intercepts $\Delta(\Delta S^{\ddagger})/R$. The values of these quantities from replicate measurements are listed in Table 4. Analogous treatment of the CAD data of AA–H^+–B_i dimers with α-alanine and the diaminoalkanes gives rise to the Eq. (10) slopes and intercepts given in Table 4; representative plots, referring to α-Ala and 1,2-diaminoethane, are illustrated in Figs. 5 and 6, respectively.

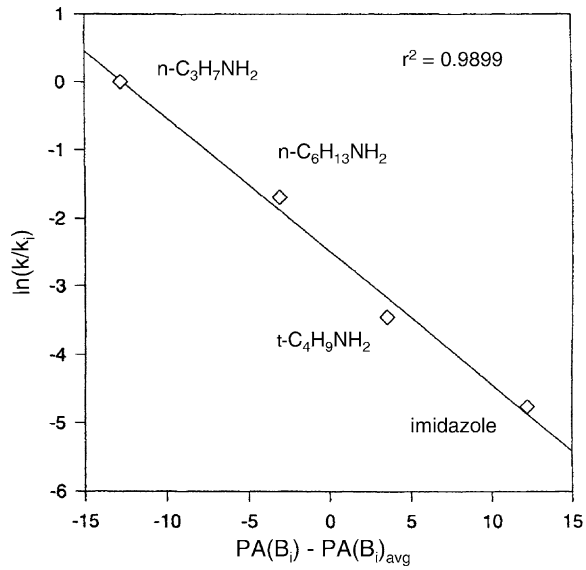

Fig. 3. Plot of $\ln(k/k_i)$ vs. $PA(B_i) - PA(B_i)_{avg}$ (Eq. (9)), for β-Ala–H^+–B_i heterodimers (B_i = *n*-propylamine, *n*-hexylamine, *t*-butylamine, imidazole) dissociating after collisional activation at a center-of-mass collision energy of 6.4 eV.

The proton affinities of the test molecules α-Ala and 1,2-diaminoethane determined in this study are in excellent agreement with those reported in the NIST database [6] (Table 5). Our value for 1,2-diaminoethane also matches within experimental error values obtained previously by Siu and co-workers [28] and

Table 2
Experimental data for β-Ala–H^+–B_i dimers (B_i = *n*-propylamine, *n*-hexylamine, *t*-butylamine, imidazole)[a]

E_{cm} (eV)	$1/RT_{eff}$ (mol kJ^{-1})[b]	T_{eff} (K)	$[GB^{app} - PA(B_i)_{avg}]/RT_{eff}$[c]	$GB^{app} - PA(B_i)_{avg}$ (kJ mol^{-1})[d]
5.5	0.279 (0.006)	432 (9)	−2.830 (0.017)	−10.2 (0.2)
5.9	0.239 (0.005)	504 (11)	−2.769 (0.015)	−11.6 (0.3)
6.4	0.196 (0.004)	614 (11)	−2.486 (0.011)	−12.7 (0.2)
6.8	0.166 (0.003)	726 (12)	−2.459 (0.013)	−14.8 (0.3)
7.2	0.148 (0.003)	812 (17)	−2.450 (0.014)	−16.5 (0.4)
7.6	0.122 (0.004)	987 (36)	−2.338 (0.020)	−19.2 (0.7)

The values in parenthesis give the corresponding standard deviations.
[a] $PA(B_i)_{avg} = 930.6$ kJ mol^{-1}. $\Delta S_H(B_i)_{avg} = 113.9$ J mol^{-1} K^{-1}.
[b] Negative slope of Eq. (9).
[c] Intercept of Eq. (9).
[d] Intercept divided by negative slope.

Holmes and co-workers [29] via the extended kinetic method (Table 5). It is noteworthy that both reference base sets used for α-Ala and 1,2-diaminoethane lead to the same PA (Table 5). Ab initio calculations have shown that the most stable structures of protonated α-Ala [41] and 1,2-diaminoethane [28] contain weak hydrogen bonds between an ammonium center and an adjacent basic group (Scheme 2); the lengths of these bonds, 2.5 Å in protonated α-Ala vs. 1.87 Å in protonated diaminoethane, point out that carbonyl substituents are less suitable electron donors for intramolecular H-bonds than amine groups. Our results with α-Ala and diaminoethane attest that the extended kinetic method provides precise proton affinities for multifunctional bases which can develop weak hydrogen bonds in their protonated forms.

For β-Ala, identical proton affinities are obtained using amine or amino acid reference bases (Table 5). The mean value from both B_i sets, 927 kJ mol^{-1}, is 25 kJ mol^{-1} higher than PA(α-Ala); hence, β-amino acids are significantly more basic molecules than isomeric α-amino acids. One can view α-Ala, β-Ala and 1,2-diaminoethane as substituted ethylamines. Comparison of their proton affinities (Table 5) to that of ethylamine ($CH_3CH_2NH_2$; PA = 912 kJ mol^{-1} [6]) indicates that introduction of a COOH (carboxyl) group at the α-carbon of ethylamine lowers the proton affinity by 10 kJ mol^{-1}, while introduction of COOH or NH_2 at the β-position increase the PA by 15 or 32 kJ mol^{-1}, respectively. The increase in PA from α-Ala to β-Ala is attributed to a decreased electron-withdrawing from NH_2 by a COOH group in β-position and a better hydrogen bonding with this arrangement (Scheme 2) [9]. The increase in PA upon the transformation $CH_3CH_2NH_2 \rightarrow$ β-Ala, as compared to the decrease observed upon $CH_3CH_2NH_2 \rightarrow$

Table 3
Experimental data for β-Ala–H^+–B_i dimers (B_i = cysteine, valine, threonine, methionine)[a]

E_{cm} (eV)	$1/RT_{eff}$ (mol kJ^{-1})[b]	T_{eff} (K)	$[GB^{app} - PA(B_i)_{avg}]/RT_{eff}$[c]	$GB^{app} - PA(B_i)_{avg}$ (kJ mol^{-1})[d]
4.4	0.151 (0.005)	798 (25)	1.545 (0.020)	10.3 (0.4)
4.9	0.147 (0.005)	821 (26)	1.498 (0.019)	10.2 (0.4)
5.4	0.135 (0.004)	890 (26)	1.325 (0.016)	9.8 (0.3)
5.9	0.117 (0.003)	1031 (25)	1.127 (0.011)	9.7 (0.3)
6.4	0.099 (0.002)	1219 (26)	0.943 (0.008)	9.6 (0.2)
6.9	0.091 (0.002)	1329 (25)	0.856 (0.007)	9.5 (0.2)

The values in parenthesis give the corresponding standard deviations.
[a] $PA(B_i)_{avg} = 917.9$ kJ mol^{-1}. $\Delta S_H(B_i)_{avg} = 113.9$ J mol^{-1} K^{-1}.
[b] Negative slope of Eq. (9).
[c] Intercept of Eq. (9).
[d] Intercept divided by negative slope.

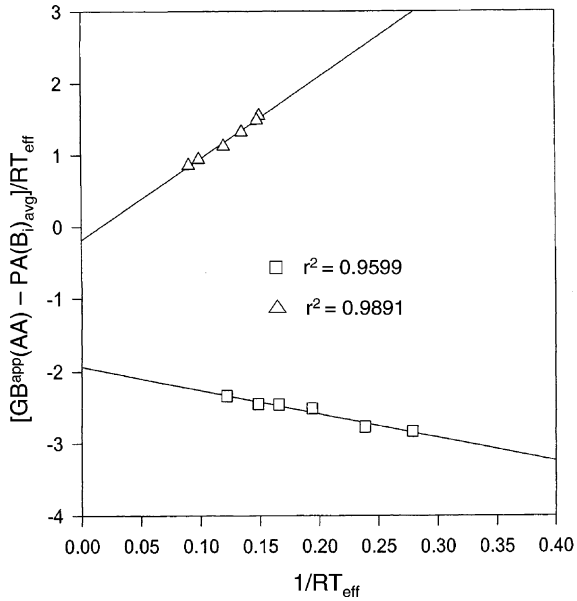

Fig. 4. Plots of $[GB^{app} - PA(B_i)_{avg}]/RT_{eff}$ vs. $1/RT_{eff}$ (Eq. (10)), for the dissociations of β-Ala–H^+–B_i heterodimers: (□), B_i = *n*-propylamine, *n*-hexylamine, *t*-butylamine, imidazole; (△), B_i = cysteine, valine, threonine, methionine.

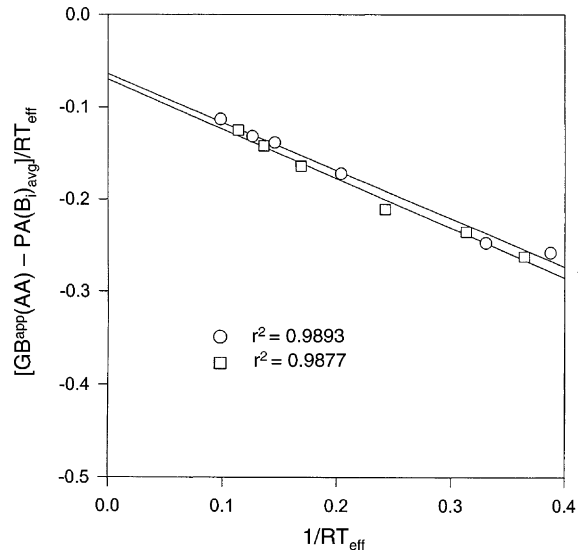

Fig. 5. Plots of $[GB^{app} - PA(B_i)_{avg}]/RT_{eff}$ vs. $1/RT_{eff}$ (Eq. (10)), for the dissociations of α-Ala–H^+–B_i heterodimers: (○), B_i = propargylamine, methylamine, allylamine, benzylamine; (□), B_i = glycine, cysteine, aspartic acid, valine.

Table 4
Thermochemical data for AA–H^+–B_i dimers

B_i[a]	$PA(B_i)_{avg}$ (kJ mol^{-1})[a]	$\Delta S_H(B_i)_{avg}$ (J mol^{-1} K^{-1})[a]	$PA(AA) - PA(B_i)_{avg}$ (kJ mol^{-1})[b,c]	$\Delta(\Delta S^{\ddagger})/R$ (kJ mol^{-1})[c,d]
β-Alanine				
Amines	930.6	113.9	−3.5 (0.5)	−1.9 (0.1)
Amino acids	917.6	113.9	10.0 (0.8)	−0.1 (0.1)
α-Alanine				
Amines	902.3	114.1	−0.7 (0.3)	−0.1 (0.1)
Amino acids	902.3	114.4	−0.8 (0.2)	−0.1 (0.1)
1,2-Diaminoethane				
Amines	946.3	112.1	3.2 (0.4)	−2.2 (0.1)
Amino acids	935.6	113.4	16.9 (1.2)	−0.8 (0.2)
1,3-Diaminopropane				
Secondary amines	972.6	111.1	1.9 (0.5)	−0.6 (0.1)
Tertiary amines	981.3	103.7	−0.8 (0.3)	−2.9 (0.1)
1,4-Diaminobutane				
Tertiary amines	990.4	103.6	2.5 (0.2)	−1.9 (0.1)

The values in parenthesis give the corresponding standard deviations.

[a] See Table 1.

[b] Slope of Eq. (10).

[c] Average values (and pooled standard deviations) from four plots according to Eq. (10) for β-Ala–H^+–amine dimers and from two plots for the dimers containing β-Ala, α-Ala and 1,2-diaminoethane.

[d] Intercept of Eq. (10).

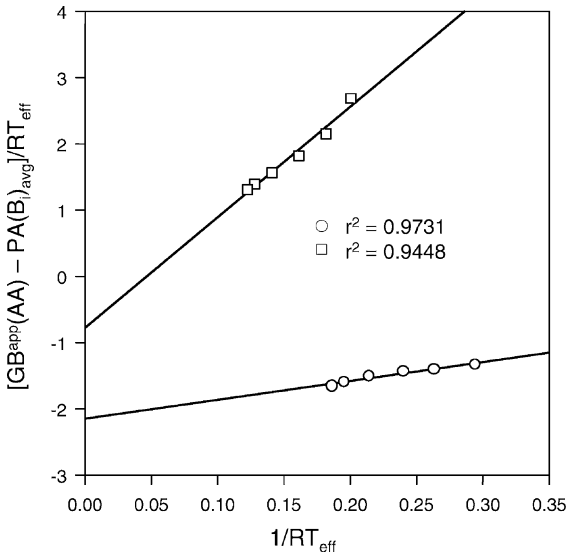

Fig. 6. Plot of $[GB^{app} - PA(B_i)_{avg}]/RT_{eff}$ vs. $1/RT_{eff}$ (Eq. (10)), for the dissociations of AA–H^+–B_i heterodimers with AA = 1,2-diaminoethane: (○), B_i = *n*-hexylamine, imidazole, diethylamine, di-*n*-propylamine; (□), B_i = threonine, methionine, tryptophan.

α-Ala further means that the stabilization provided by H-bonding in protonated β-Ala outweighs the destabilization incurred by the inductive effect of the COOH group. Replacing the COOH group of β-Ala with an NH_2 group leads to 1,2-diaminoethane; this molecule has an even higher PA because of the lesser electron-withdrawing character of amine vs. carboxyl substituents, and the higher basicity of a β-NH_2 vis-à-vis a β-COOH group which leads to a stronger H-bond.

Two reference base sets with markedly different average protonation entropies could be used in the determination of the proton affinity of 1,3-diaminopropane (Tables 1 and 5). The PA resulting from dimers with secondary amines as B_i molecules is lower than the PA obtained with tertiary amines (Table 5). The mean value from these experiments, 978 ± 4 kJ mol^{-1}, lies slightly below the PA reported by NIST, 987 kJ mol^{-1} [6], but is very similar to the PA measured by Siu and co-workers using Eqs. (6)–(8) of the extended

Table 5
Proton affinities (PAs, kJ mol^{-1}) of molecules studied

AA	B_i	PA(AA)	
		This study[a]	Literature
β-Alanine	Amines	927.1	
	Amino acids	927.6	
	Mean	927 (4)	
α-Alanine	Amines	901.6	
	Amino acids	901.5	
	Mean	902 (4)	902[b]
1,2-Diaminoethane	Amines	949.5	
	Amino acids	952.5	
	Mean	951 (4)	952[b], 948[c], 949[d]
1,3-Diaminopropane	Secondary amines	974.5	
	Tertiary amines	980.5	
	Mean	978 (4)	987[b], 982[c], 967[d]
1,4-Diaminobutane	Tertiary amines	993 (4)	1006[b], 1010[c], 974[d]

[a] Obtained by adding the relative affinities listed in Table 4 to $PA(B_i)_{avg}$; mean values are also given if more than one heterodimer series were used. The numbers in parenthesis are the compounded uncertainties in relative values (Table 4) and $PA(B_i)_{avg}$ (±4 kJ mol^{-1} or better [6]).

[b] NIST database [6].

[c] Ref. [28], using extended kinetic method (Eqs. (6)–(8)), at 3–4 collision energies (lower limit).

[d] Ref. [29], using extended kinetic method (Eqs. (6)–(8)), with metastable and collisionally activated dimer ions (lower limit).

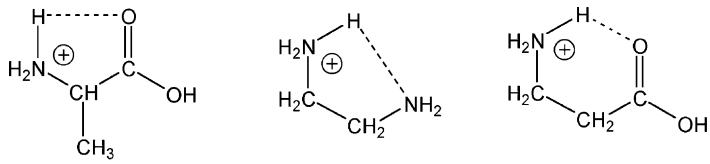

Scheme 2.

kinetic method at three different effective temperatures (982 kJ mol^{-1}) [28]. A lower value, viz. 967 kJ mol^{-1}, was found by Holmes and co-workers, based on AA–H$^+$–B$_i$ dimer dissociations at only two different effective temperatures [29]. With 1,4-diaminobutane, the most basic test molecule studied [6], only one reference base set could be used, viz. the tertiary amines given in Table 1. Our PA with this B$_i$ set (993 ± 4 kJ mol^{-1}, Table 5) is again somewhat lower than the PA listed in the NIST database (1006 kJ mol^{-1}) [6]. In this case, Siu and co-workers reported a higher value (1010 kJ mol^{-1}) [28], while Holmes and co-workers, reported a considerably lower value (974 kJ mol^{-1}) [29].

Ab initio calculations predict that protonated 1,3-diaminopropane and 1,4-diaminobutane (Scheme 3) form much stronger hydrogen bonds than protonated 1,2-diaminoethane (Scheme 2) [28,42,43]. This is evident from the calculated $H_2NH^+ \cdots N$ bond lengths and N^+–H $\cdots$ N bond angles which are 1.87 Å/124°, 1.65 Å/150° and 1.61 Å/173° in the protonated 1,2-, 1,3- and 1,4-diaminoalkane, respectively [28]; generally, the shorter the H-bond and the closer to 180° the corresponding angle, the stronger the hydrogen bonding interaction [42,43]. Our results concur with

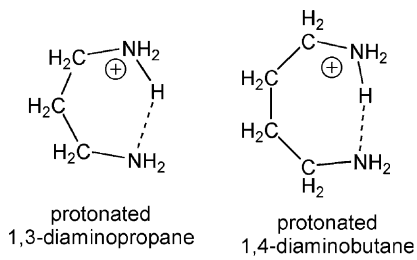

Scheme 3.

the conclusions reached previously by Holmes and co-workers [29] that the extended kinetic method underestimates the proton affinities of difunctional molecules which form strong hydrogen bonds after protonation (such as 1,3-diaminopropane and 1,4-diaminobutane). Comparison of our PAs to those of Holmes and co-workers, also reveals that the underestimation is less severe when the entropy correction is based on data from six (or more) different internal energies (Tables 2–3 and Figs. 4–6) than on data from just two internal energies [29]. (In this latter case, the entropy correction is appraised from the position of the intersection point of the two lines derived via Eq. (6) from metastable and collisionally activated heterodimer ions [29].)

The underestimation of PAs for molecules that form strong hydrogen bonds in their protonated forms could originate from (a) the presence of a reverse activation energy (E_{rev}) in the dissociation AA–H$^+$–B$_i$ → AA–H$^+$ + B$_i$ (where AA–H$^+$ is the strongly hydrogen-bonded species) and/or (b) an underestimation of $\Delta(\Delta S^{\ddagger})$ in these instances. The relative entropy term is discussed later.

A reverse activation energy provides excess energy to the transition state leading to AA–H$^+$ + B$_i$; if a substantial fraction of this energy is transferred into translational energy of the products, a common means of E_{rev} disposal, large kinetic energy releases ($T_{0.5}$) would be observed for the AA–H$^+$ fragments (in tandem mass spectra acquired at keV kinetic energies and with an electrostatic analyzer as the mass separating device) [38–40]. The kinetic energy releases accompanying the formation of protonated 1,3-diaminopropane and 1,4-diaminobutane from metastable proton-bound dimers are, however, small (see Section 3.2), as are the

kinetic energy releases associated with the fragments from all other AA–H^+–B_i heterodimers examined. Holmes and co-workers [29] and Lund and Bojesen [44] made similar observations. A small kinetic energy release does not necessarily preclude a reverse energy barrier. The rovibronic coupling between the electrostatically bound species in AA–H^+–B_i could be weak, such that there is no clearly defined reaction coordinate for their separation. Under these conditions, the excess energy of the dissociating transition state may not be significantly partitioned into translational degrees of freedom of the products, but could instead be dissipated into their rovibrational degrees of freedom [45,46]. If the amount, by which the PAs of 1,3-diaminopropane and 1,4-diaminobutane are underestimated, is assumed to be equal with E_{rev}, the reverse barriers are quite small ($\leq$13 kJ mol^{-1}, cf. Table 5) and would have little impact on the tandem mass spectra of the corresponding heterodimers. Overall, the experimental data would be consistent with but do not conclusively prove the existence of E_{rev} in the decomposition of proton-bound dimers of 1,3-diaminopropane and 1,4-diaminobutane; quantum chemistry methods are necessary to unequivocally solve this problem.

3.4. Relative entropies from the extended kinetic method

For α-Ala, the $\Delta(\Delta S^{\ddagger})$ values furnished by the extended kinetic method match within experimental error the relative protonation entropies of the bases compared in the respective AA–H^+–B_i dimers (Table 6). This is also true for the heterodimers of 1,2-diaminoethane with amines; in contrast, the heterodimers of 1,2-diaminoethane with amino acids lead to a significantly smaller $\Delta(\Delta S^{\ddagger})$. Also for 1,3-diaminopropane and 1,4-diaminobutane (Table 6), the experimentally deduced $\Delta(\Delta S^{\ddagger})$ amounts lie below $\Delta(\Delta S_H) = \Delta S_H(AA) - \Delta S_H(B_i)$. The results for β-Ala follow the same trend as those for 1,2-diaminoethane, viz. different $\Delta(\Delta S^{\ddagger})$ values are obtained using amines or amino acids as reference bases (cf. Table 6). Again, $\Delta(\Delta S^{\ddagger})$ is markedly smaller with amino acid than amine B_i molecules, even though these B_i sets have comparable average $\Delta S_H(B_i)$ values (Table 1); despite such discrepancy in $\Delta(\Delta S^{\ddagger})$, however, both sets yield identical proton affinities (Table 5).

$\Delta(\Delta S^{\ddagger})$ is deduced by probing the competitive dissociations of AA–H^+–B_i at different collision energies, each corresponding to a distinct mean internal

Table 6
Comparison of relative entropies from extended kinetic method, $\Delta(\Delta S^{\ddagger})$, with the relative protonation entropies of the bases compared in the heterodimers, $\Delta(\Delta S_H) = \Delta S_H(AA) - \Delta S_H(B_i)$

AA	B_i[a]	$-\Delta(\Delta S^{\ddagger})$ (J mol^{-1} K^{-1})[b]	$\Delta(\Delta S_H)$ (J mol^{-1} K^{-1})[c]	$(T_{eff})_{avg}/(E_{cm})_{avg}$ (K eV^{-1})[d]
β-Alanine	Amines	16		103
	Amino acids	1		180
α-Alanine	Amines	1	0	102
	Amino acids	1	−1	100
1,2-Diaminoethane	Amines	18	19	69
	Amino acids	7	19	188
1,3-Diaminopropane	Secondary amines	5	47	93
	Tertiary amines	24	54	87
1,4-Diaminobutane	Tertiary amines	16	69	89

[a] See Table 1 for B_i sets used.
[b] This study, ±1 J mol^{-1} K^{-1} (cf. Table 4).
[c] Calculated from PA and GB data given in [6]. See Table 4 for average $\Delta S_H(B_i)$.
[d] Mean of effective temperatures sampled in CAD experiments, normalized by mean of the corresponding collision energies (see Tables 2 and 3 for actual T_{eff} and E_{cm} values of dimers composed of β-Ala and either amines or amino acids).

energy and effective temperature (vide supra). The mean value of the various T_{eff} sampled by a series of AA–H^+–B_i dimers, divided by the mean value of the corresponding center-of-mass collision energies, $(T_{eff})_{avg}/(E_{cm})_{avg}$, can be used as a qualitative measure of the average internal energies of the dissociating dimers; these normalized average effective temperatures are included in Table 6. The relationship between $(T_{eff})_{avg}/(E_{cm})_{avg}$ and $\Delta(\Delta S^{\ddagger})$ for α-Ala, β-Ala, 1,2-diaminoethane and 1,3-diaminopropane, i.e., the molecules which could be paired with two different types of reference bases (Table 1), unveils some useful insight about the nature of $\Delta(\Delta S^{\ddagger})$, as presented here.

Both types of α-Ala–H^+–B_i dimers show the same normalized $(T_{eff})_{avg}$ and also yield the same $\Delta(\Delta S^{\ddagger})$ (Table 6). For the AA–H^+–B_i dimers of β-Ala, 1,2-diaminoethane and 1,3-diaminopropane, on the other hand, distinct $(T_{eff})_{avg}/(E_{cm})_{avg}$ and $\Delta(\Delta S^{\ddagger})$ values are observed with the two B_i sets used; in all three cases, the B_i set associated with the higher normalized effective temperature gives rise to a smaller $\Delta(\Delta S^{\ddagger})$. Evidently, as the internal energy distribution of AA–H^+–B_i shifts toward higher average internal energies (and thus, higher T_{eff}), the relative entropy decreases. Such a trend, viz. a $\Delta(\Delta S^{\ddagger})$/internal energy correlation provides credence to the conclusion of Ervin that the relative entropies measured by the extended kinetic method are proportional to the logarithm of the ratio of the microcanonical sum of states of the dissociation transition states *at the kinetically selected internal energy distribution of the dissociating ions* [22]. Changing the internal energy distribution (by changing the B_i set) affects this ratio, which should in turn alter $\Delta(\Delta S^{\ddagger})$, as indeed observed. Ervin's study concerned specifically metastable ion fragmentations [22], while our study focuses on collisionally activated dissociations. Internal energy distributions are broader upon CAD; nevertheless, the analogous findings by Ervin and us attest that the $\Delta(\Delta S^{\ddagger})$ values derived from both metastable as well as collisionally activated dimer ions are not thermodynamic relative entropies but relative entropies of the dissociating transition states at the actual (and usually non-Boltzmann) energy distribution of the dimers.

With both types of α-Ala heterodimers and the heterodimers of 1,2-diaminoethane and amines, $\Delta(\Delta S^{\ddagger})$ is found to be very similar with the thermodynamic $\Delta(\Delta S_H)$ term (vide supra); this similarity might be either coincidental or due to Boltzmann-resembling internal energy distributions of the collisionally activated heterodimer ions of these molecules. It is noteworthy that, when AA is paired with different B_i sets, the set of smaller $PA(AA) - PA(B_i)_{avg}$ results in a smaller $(T_{eff})_{avg}/(E_{cm})_{avg}$ (see corresponding entries in Tables 4 and 6, respectively). Apparently, the average internal energy deposited into AA–H^+–B_i increases with the relative proton affinity of AA vs. B_i [16–20].

Eq. (7) can be rewritten as $PA = GB^{app} - T_{eff}\Delta(\Delta S^{\ddagger})$ to more clearly show the dependence on $\Delta(\Delta S^{\ddagger})$ of the proton affinities furnished by the extended kinetic method. $\Delta(\Delta S^{\ddagger})$ is negative with the molecules studied (Table 4), leading to PAs that are higher than the corresponding GB^{app} values. For the test molecules that form relatively weak hydrogen bonds after protonation, viz. α-Ala and 1,2-diaminoethane, the $T_{eff}\,\Delta(\Delta S^{\ddagger})$ correction produces the correct proton affinity (vide supra). It is possible that the underestimation of PAs when strong H-bonds are formed after protonation (as with 1,3-diaminopropane and 1,4-diaminobutane) originates from an underestimation of the absolute value of $\Delta(\Delta S^{\ddagger})$. Note that $\Delta(\Delta S^{\ddagger})$ is assumed to be constant for a given AA–H^+–B_i series in the effective temperature range sampled at the different collision energies used in the CAD experiments. This assumption is not rigorous, however. Ervin recently showed by RRKM theory that the $\Delta(\Delta S^{\ddagger})$ value associated with the dissociations of proton-bound alkoxide dimers varies with T_{eff} [22]. Likewise, the $\Delta(\Delta S^{\ddagger})$ values of the individual reference bases within the AA–H^+–B_i set may be slightly different from each other. Both these factors could contribute to the underestimation of the proton affinities of 1,3-diaminopropane and 1,4-diaminobutane by the extended kinetic method.

4. Conclusions

The extended kinetic method is shown to yield accurate proton affinities for molecules that carry weak intramolecular interactions (hydrogen bonds) after protonation, such as α-Ala, β-Ala and 1,2-diaminoethane. In contrast, the proton affinities of species that become strongly hydrogen-bonded when protonated, such as 1,3-diaminopropane and 1,4-diaminobutane, are slightly underestimated; the underestimation is attributed to small reverse barriers in the dissociation of heterodimers of the latter molecules and/or to variations in the relative activation entropy of the competitive heterodimer dissociations during the CAD experiments.

The relative entropy derived by the extended kinetic method, $\Delta(\Delta S^{\ddagger})$, is not a thermodynamic quantity affiliated with a Boltzmann energy distribution of dissociating dimer ions, but an entropy difference related to the actual internal energy distribution of the dissociating ions, as had been predicted by the RRKM modeling of Ervin [22]. Because the internal energy deposited on a heterodimer strongly depends on experimental conditions, $\Delta(\Delta S^{\ddagger})$ data for the same set of heterodimers may vary, inter alia, with CAD conditions, the lifetime of the dimer ions and the ionization method used to produce the dimer ions.

The extended kinetic method definitely provides an improvement in measured affinities for certain molecules. Without full entropy correction, β-Ala–H^+–amine dimers would have led to PA(β-Ala) = 911–920 kJ mol^{-1}, depending on the collision energy used (see right column in Table 2) vis-à-vis the 927 ± 4 kJ mol^{-1} deduced from the extended version (Tables 4 and 5). Similarly, the proton affinity of 1,2-diaminoethane would have been undervalued by 9–14 kJ mol^{-1} with the classical kinetic method (using amine reference bases) and those of 1,3-diaminopropane and 1,4-diaminobutane, which are underestimated by the extended kinetic method (vide supra), would have been even lower without entropy correction, by up to 16 and 9 kJ mol^{-1}, respectively. On the other hand, the extended kinetic method provides no improvement for α-Ala (with either B_i set) and for β-Ala (if it is paired with amino acids), because in these cases $\Delta(\Delta S^{\ddagger})$ is negligible at the selected experimental conditions (Table 4). Since the internal energy distribution of the dissociating ions and, hence $\Delta(\Delta S^{\ddagger})$, cannot be predicted a priori, it is advisable to apply the kinetic method at several different internal energies. If the resulting GB^{app} values do not change significantly with collision energy (see, for example, right column of Table 3), there is no need to proceed with entropy corrections and the average of the apparent basicities should be reported as the PA. Conversely, if GB^{app} is found to be sensitive to the collision energy (Table 2, right column), then application of the extended kinetic method is called for, as it will lead to a more accurate PA than the classical approach.

Proton affinity is a state function and does not depend on the pathway through which it is determined. In sharp contrast, $\Delta(\Delta S^{\ddagger})$ values deduced from non-equilibrium kinetic method measurements depend on the internal energy distribution of the dissociating ions and, hence, on experimental conditions (i.e., the pathway). Because of this distinctive characteristic, an alternative means for determining the necessity of entropy corrections is to pair the molecule of interest with several different reference bases, so that a thermochemical ladder can be constructed and checked for self-consistency. For example, if A is paired with X and Y, and $\ln(k_A/k_X)$ is found equal to $\ln(k_A/k_Y) - \ln(k_Y/k_X)$, the self-consistency criterion is fulfilled (no dependence on pathway) and the extended kinetic method needs not be employed. The opposite scenario would indicate that full entropy correction via the extended kinetic method is necessary.

Acknowledgements

We are indebted to Dr. Michael J. Polce for experimental assistance and valuable scientific discussions, to Dr. Kent M. Ervin for helpful comments and to Dr. Peter B. Armentrout for kindly providing us the software for the statistical treatment of the experimental results from the extended kinetic method. We thank

the National Science Foundation (CHE-0111128) for generous financial support.

References

[1] G. Zubay, Biochemistry, 2nd ed., MacMillan, New York, 1988.
[2] (a) K. Biemann, S.A. Martin, Mass Spectrom. Rev. 6 (1987) 1;
(b) I.A. Papayannopoulos, Mass Spectrom. Rev. 14 (1995) 49.
[3] J.R. Chapman (Ed.), Protein and Peptide Analysis by Mass Spectrometry, Humana Press, Totowa, NJ, 1996.
[4] M. Kinter, N.E. Sherman, Protein Sequencing and Identification Using Tandem Mass Spectrometry, Wiley-Interscience, New York, 2000.
[5] A.G. Harrison, Mass Spectrom. Rev. 16 (1997) 201.
[6] E.P.L. Hunter, S.G. Lias, J. Phys. Chem. Ref. Data 27 (1998) 413.
[7] A.E. Pojitkov, E.N. Efremenko, S.D. Varfolomeev, J. Mol. Cat. B: Enzym. 10 (2000) 47.
[8] D. Seebach, J.L. Matthews, Chem. Commun. (1997) 2015.
[9] J. Wu, E. Gard, J. Bregar, M.K. Green, C.B. Lebrilla, J. Am. Chem. Soc. 117 (1995) 9900.
[10] R.G. Cooks, J.S. Patrick, T. Kotiaho, S.A. McLuckey, Mass Spectrom. Rev. 13 (1994) 287.
[11] R.G. Cooks, P.S.H. Wong, Acc. Chem. Res. 31 (1998) 379.
[12] X. Cheng, Z. Wu, C. Fenselau, J. Am. Chem. Soc. 115 (1993) 4844.
[13] M.J. Nold, B.A. Cerda, C. Wesdemiotis, J. Am. Soc. Mass Spectrom. 10 (1999) 1.
[14] P.J. Robinson, K.A. Holbrook, Unimolecular Reactions, Wiley-Interscience, London, 1972.
[15] K.J. Laidler, Chemical Kinetics, 3rd ed., Harper & Row, Cambridge, 1987, p. 112.
[16] L. Drahos, K. Vékey, J. Mass Spectrom. 34 (1999) 79.
[17] R.G. Cooks, J.T. Koskinen, P.D. Thomas, J. Mass Spectrom. 34 (1999) 85.
[18] K.M. Ervin, Int. J. Mass Spectrom. 195/196 (2000) 271.
[19] S. Campbell, E.M. Marzluff, M.T. Rodgers, J.L. Beauchamp, M.E. Rempe, K.F. Schwinck, D.L. Lichtenberg, J. Am. Chem. Soc. 116 (1994) 5257.
[20] S.L. Craig, M. Zhong, J.I. Brauman, J. Phys. Chem. A 101 (1997) 19.
[21] P.B. Armentrout, J. Mass Spectrom. 34 (1999) 74.
[22] K.M. Ervin, J. Am. Soc. Mass Spectrom. 13 (2002) 435.
[23] Z. Wu, C. Fenselau, Rapid Commun. Mass Spectrom. 8 (1994) 777.
[24] B.A. Cerda, C. Wesdemiotis, J. Am. Chem. Soc. 118 (1996) 11884.
[25] B.A. Cerda, S. Hoyau, G. Ohanessian, C. Wesdemiotis, J. Am. Chem. Soc. 120 (1998) 2437.
[26] B.A. Cerda, C. Wesdemiotis, Int. J. Mass Spectrom. 185–187 (1999) 107.
[27] B.A. Cerda, C. Wesdemiotis, Int. J. Mass Spectrom. 189 (1999) 189.
[28] Z. Wang, I.K. Chu, C.F. Rodriquez, A.C. Hopkinson, K.W.M. Siu, J. Phys. Chem. A 103 (1999) 8700.
[29] J. Cao, C. Aubry, J.L. Holmes, J. Phys. Chem. A 104 (2000) 10045.
[30] P.B. Armentrout, J. Am. Soc. Mass Spectrom. 11 (2000) 371.
[31] P.G. Wenthold, J. Am. Soc. Mass Spectrom. 11 (2000) 601.
[32] T.I. Williams, J.W. Denault, R.G. Cooks, Int. J. Mass Spectrom. 210/211 (2001) 133.
[33] N. Morlender-Vais, J.L. Holmes, Int. J. Mass Spectrom. 210/211 (2001) 147.
[34] L. Di Donna, A. Napoli, G. Sindona, Int. J. Mass Spectrom. 210/211 (2001) 165.
[35] A.F. Kuntz, A.W. Boynton, G.A. David, K.E. Kolyer, J.C. Poutsma, J. Am. Soc. Mass Spectrom. 13 (2002) 72.
[36] J. Laskin, J.H. Futrell, J. Phys. Chem. 104 (2000) 8829.
[37] M.J. Polce, M.M. Cordero, C. Wesdemiotis, P.A. Bott, Int. J. Mass Spectrom. Ion Process. 113 (1992) 35.
[38] K.L. Busch, G.L. Glish, S.A. McLuckey, Mass Spectrometry/Mass Spectrometry: Techniques and Applications of Tandem Mass Spectrometry, VCH, New York, 1988.
[39] R.G. Cooks, J.H. Beynon, R.M. Caprioli, G.R. Lester, Metastable Ions, Elsevier, Amsterdam, 1973.
[40] (a) J.L. Holmes, J.K. Terlouw, Org. Mass Spectrom. 15 (1980) 383;
(b) J.L. Holmes, Org. Mass Spectrom. 20 (1985) 169.
[41] C.J. Cassady, S.R. Carr, K. Zhang, A. Chang-Phillips, J. Org. Chem. 60 (1995) 1704.
[42] S. Yamabe, K. Hirao, H. Wasada, J. Phys. Chem. 96 (1992) 10261.
[43] G. Bouchoux, N. Choret, F. Berruyer-Penaud, J. Phys. Chem. A 105 (2001) 3989.
[44] K.H. Lund, G. Bojesen, Int. J. Mass Spectrom. 156 (1996) 203.
[45] S.T. Graul, M.T. Bowers, J. Am. Chem. Soc. 113 (1991) 9696.
[46] S.T. Graul, M.T. Bowers, J. Am. Chem. Soc. 116 (1994) 3875.